

## Magnetic Phase Diagram of the UAs-US System\*

G. H. Lander, M. H. Mueller, and J. F. Reddy

*Materials Science Division, Argonne National Laboratory, Argonne, Illinois 60439*

(Received 29 November 1971)

The magnetic phase diagram of the  $\text{UAs}_{1-x}\text{S}_x$  system ( $0 \leq x \leq 1$ ) has been investigated by neutron diffraction with powder samples. The solid solutions are face-centered cubic (NaCl crystal structure), and the anion atoms are distributed randomly over the anion sublattice. For  $x=0$  (UAs), the type-I antiferromagnetic ordering ( $T_N=127$  K), consisting of ferromagnetic sheets stacked  $+ - + -$ , changes at  $0.5T_N$  to the type-IA ordering, in which the sheets are stacked  $++--$ . This transition is accompanied by an abrupt increase in the magnetic moment from 1.9 to  $2.2\mu_B$  per uranium atom. As  $x$  increases from zero, the stability of the type-IA structure increases until for  $x=0.20$  this phase is present at all temperatures below  $T_N$ . For  $x$  between 0.25 and 0.34 the magnetic moments are not arranged in a simple commensurate structure, but their modulation from layer to layer follows a sinusoidal form. Near  $T_N$ , a single harmonic is present: The repeat distance in real space varies from  $\sim 2.8$  unit cells at  $x=0.25$  to  $\sim 4.2$  unit cells at  $x=0.34$ . A third harmonic, implying some squaring of the sine wave, appears at about  $0.5T_N$ . The periodicity is a function of concentration ( $x$ ) only and does not vary with temperature for a given sample. Although at the ends of this intermediate range the stable phases at low temperature tend to be either type IA (low  $x$ ) or ferromagnetic (high  $x$ ), the longitudinal-wave structure is stable to at least 2.2 K over a narrow composition range.

### I. INTRODUCTION

The difficulties in understanding the magnetism of the  $5f$  (actinide) series are increased by the absence of any spontaneous magnetism in the first three elements, uranium, neptunium, and plutonium. However, many compounds of these elements are magnetically ordered, and one of the simplest groups is the mononictides and monochalcogenides [i. e., one-to-one compounds with elements of group VA (phosphorus, arsenic) and group VIA (sulfur, selenium), respectively] that have the NaCl crystal structure. Much of the work on the uranium compounds has been reviewed,<sup>1</sup> but an understanding of the magnetic behavior is far less complete than that presented in even the early studies<sup>2</sup> on analogous lanthanide compounds. For the most part these complexities may be attributed to the large crystal fields and exchange interactions in the actinide compounds. In the octahedral field applicable to the UX-type compounds, the fourth-order crystal field potential is at least an order of magnitude greater than in the comparable lanthanide compounds. The spin-orbit coupling is of comparable energy, leading to the consideration of intermediate coupling schemes, with all the concomitant complications. The magnetic ordering temperatures in these compounds are usually above 100 K, but in the LnX compounds seldom exceed 30 K. The exchange interactions are therefore larger in the actinide series, but their precise magnitude remains a speculative matter. Additional evidence that the exchange mechanism is long range and of the Ruderman-Kittel-Kasuya-Yosida (RKKY) type has been implied from the neutron in-

vestigation of the UP-US solid solutions,<sup>3,4</sup> in which magnetic structures were found with periodicities that extended over several unit cells. In many cases compounds form solid solutions with each other, with the anion (or cation) distributed randomly over the respective sublattice. In the case of uranium compounds, U VA are antiferromagnetic, whereas U VIA are ferromagnetic, so that the solid solutions make excellent systems for studying the competing ferro- and antiferromagnetic exchange interactions. Numerous papers have been published on the UP-US system covering the neutron,<sup>3,4</sup> NMR,<sup>5,6</sup> and x-ray work.<sup>7</sup> In the present neutron-diffraction study we have examined the UAs-US solid solutions. UAs, like UP, is antiferromagnetic and forms a complete range of solid solutions with US, which is ferromagnetic. Studies of UAs<sup>8-11</sup> indicate that at low temperatures it has the type-IA ordering, and its behavior is therefore similar to low-sulfur-concentration compounds in the UP-US system, e. g.,  $\text{UP}_{0.92}\text{S}_{0.08}$ . Strong similarities between the two systems should exist, leading to a better explanation of the magnetic properties in terms of electron concentration.

### II. EXPERIMENTAL

As described by Baskin,<sup>12</sup> UAs was prepared by reacting powdered uranium with  $\text{AsH}_3$  at 300 °C. The resulting  $\text{UAs}_2$ , which is pyrophoric, was reduced at 1400 °C to obtain UAs. The major contaminant was  $\text{UO}_2$ , and both x-ray and neutron patterns indicated that small amounts ( $\sim 2\%$ ) of  $\text{UO}_2$  were present in the early batches of UAs. No other impurities were detected by x-ray, neutron, or chemical analysis. In the later batches of UAs

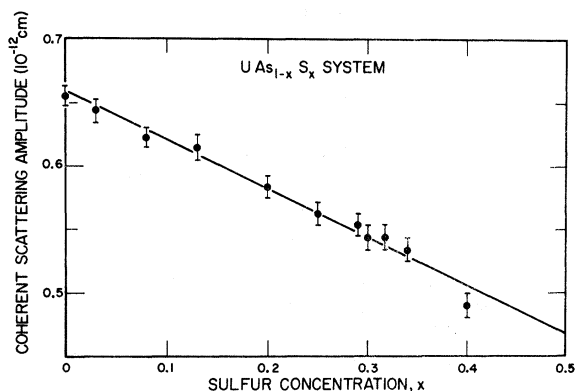


FIG. 1. Coherent scattering amplitude of the (As, S) site in the NaCl crystal structure relative to that of uranium ( $b_U = 0.85 \times 10^{-12}$  cm).

the  $UO_2$  contamination was reduced; experiments have shown that the magnetic phase diagram is insensitive to this impurity. The compounds were prepared by weighing the correct proportions of UAs with high-purity US prepared previously in this laboratory, ball-milling for 16 h, and pressing the pellets in a 0.4-in.-diam steel die under 40 000 psi. No binder was necessary. The pellets were then fired at 1600 °C for 3 h. The lattice parameters, as determined from x-ray powder patterns, follow closely the results given by Baskin.<sup>12</sup> The values for UAs and US are 5.779 and 5.490 Å, respectively. Inasmuch as UP has a lattice parameter of 5.589 Å, the uranium-to-uranium distance ( $a/\sqrt{2}$ ) is 3% greater in UAs than in UP. In the UP-US solid solutions, the lattice parameters depart slightly from linearity across the composition range, and the same is true of the UAs-US system.

Sample homogeneity in these solid solutions has been a matter of some discussion. In analysis of the linewidths in both x-ray and NMR experiments on the UP-US system,<sup>7</sup> the variations in homogeneity were of the order of  $\pm 5\%$  of the smaller anion concentration. In the UAs-US system a similar situation exists. Thus at a nominal sulfur concentration of  $x_0$ , using the notation  $UAs_{1-x}S_x$  for the solid solutions, a large polycrystalline sample will, in fact, be more truly represented by a Gaussian distribution centered on  $x_0$ , and with the 95% confidence level that includes  $x_0 \pm 0.05x_0$ . The magnetic properties will be affected by this distribution of concentrations. In particular, phase transitions, which would appear at a definite temperature if a uniform concentration were present, will occur over a temperature range. However, apart from these small variations in concentration, the anion atoms are distributed randomly over their sublattice. Experimental evidence for this is shown in Fig. 1, in which the anion scattering

length (relative to  $b_U = 0.85$ ) is plotted against the nominal sulfur concentration  $x$ . The straight line is the least-squares fit that gives  $b = 0.658 \pm 0.005$  at  $x = 0$  (i. e.,  $b_{As}$ ), and  $b = 0.277 \pm 0.016$  at  $x = 1$  (i. e.,  $b_S$ ). The published values are  $b_{As} = 0.64 \pm 0.01$  and  $b_S = 0.2847 \pm 0.0001$ .<sup>13</sup> (All scattering lengths are in units of  $10^{-12}$  cm.)

The neutron experiments were performed with a standard two-circle powder diffractometer. A monochromatic beam of  $\lambda = 1.218$ -Å neutrons was obtained with the (111) reflection from a germanium crystal. Second-order contamination, ideally absent for this reflection, was eliminated by rotating the monochromating crystal to avoid positions of multiple scattering. Soller collimation, both before and after the sample, gave diffraction peaks with full width at half-maximum (FWHM) of  $0.62^\circ$  over the angular region of interest, 15 to  $30^\circ$  in  $2\theta$ . The samples were contained in helium-filled  $\frac{7}{16}$ -in.-diam vanadium capsules, approximately 1.5 in. long. The exchange-gas Janis cryostat provided temperature control between 2.5 and 320 K. Temperature was measured with calibrated resistors composed of platinum for above 30 K and of germanium for below.

The magnetic form factor of uranium is of interest in any discussion of the electronic structure, but the present experiments have essentially been restricted to low-angle reflections, and previously reported values<sup>4</sup> have been used.

#### A. Compositions $0 \leq x \leq 0.20$

In this region, five samples with  $x = 0.0, 0.03, 0.08, 0.13,$  and  $0.20$  have been examined. For UAs ( $x = 0$ ), neutron experiments<sup>9,11</sup> have established that (i)  $T_N = 127$  K; (ii) the moments at 78 and 4 K are  $1.93$  and  $2.20$  (each  $\pm 0.05$ )  $\mu_B$ , respectively; and (iii) at  $66 \pm 1$  K, the type-I magnetic structure transforms to the type-IA structure, which is then stable at low temperatures. In the type-IA structure, ferromagnetic (001) sheets are directed along the  $c$  axis in the sequence  $++--$ , rather than in the simple alternating sequence  $+--+$ , which forms the type-I structure found in UP and other NaCl-type uranium compounds. Our own experiments on UAs are in excellent agreement with the previous work; but, in addition, we note that the magnitude of the magnetic moment changes abruptly at the type-I-type-IA transition, which is illustrated in Fig. 2. Between 85 and 70 K (at 70 K,  $T/T_N = 0.55$ ), the moment per uranium atom is essentially constant at  $1.92\mu_B$ , but after the full development of the type-IA structure the moment is  $2.24\mu_B$ , and remains unchanged on cooling to 5 K. The transition temperature is estimated at  $63 \pm 2$  K, compared with  $66 \pm 1$  K in Ref. 11. The increase in moment in UAs may be also derived from Fig. 1 of Ref.

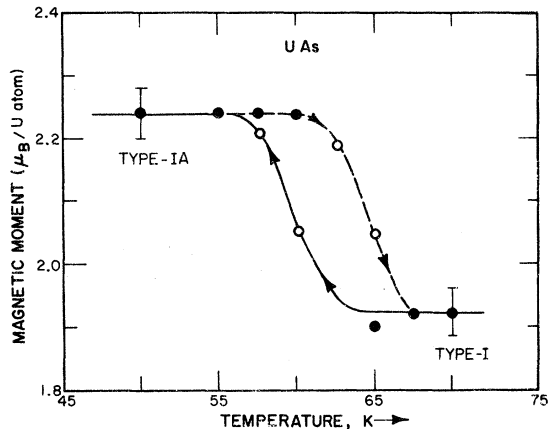


FIG. 2. Root-mean-square (rms) magnetic moment per uranium atom in UAs in the temperature range 45–75 K. Open circles indicate that both the type-I and type-IA magnetic structures were observed. The rms moment, i. e.,  $\mu = (\mu_I^2 + \mu_{IA}^2)^{1/2}$ , lies in the region 1.92–2.24  $\mu_B$  when both phases are present. However, the local moment per uranium atom is probably either 1.92  $\mu_B$ , if the structure is type I, or 2.24  $\mu_B$ , if it is type IA.

11. In comparison with the (110) reflection (type I) the product of the Lorentz factor, magnetic interaction vector, and form factor is decreased (by  $\sim 23\%$ ) for the first magnetic reflection of type IA. Hence for equal intensities—as this figure illustrates—the moment per uranium atom must be increased. The nature of the transition in UAs is of considerable interest. In UP both neutron<sup>14</sup> and NMR<sup>15</sup> measurements show that the “moment jump” at 22 K occurs over a narrow temperature range. Long and Wang<sup>16</sup> have proposed that this first-order transition results from crossings of the crystal-field levels when the Hamiltonian contains electric-quadrupole interactions that arise both from the large unquenched orbital moments and from the usual molecular-field terms. A similar situation may occur in UAs, except that this transition also involves a change in the magnetic ordering. No critical scattering was observed at the type-I–type-IA transition, as opposed to the large amount observed at the Néel temperature, which suggests that the low-temperature transition is of first order. On the other hand, the type-I–type-IA transition occurs over a relatively wide temperature range (Fig. 2) and, in the case of stoichiometric UAs, this cannot be ascribed to sample inhomogeneity.<sup>7</sup> Experimentally, a transition width of 2–3 deg could be ascribed to temperature differences across the large ( $\sim 15$  g) polycrystalline sample. However, no appreciable thermal hysteresis was detected at the Néel temperature (127 K), and the hysteresis of the transition from type-I to type-IA illustrated in Fig. 2 is therefore unlikely to arise wholly from experi-

mental effects.

For  $x = 0.03$  the Néel temperature remains the same as in UAs, but the transition from the type-I to the type-IA magnetic structure occurs at 81 K, 18 K higher than in UAs. As in UAs, the transition extends over  $\sim 10$  K. For  $x = 0.08$  the type-I–type-IA transition occurs above 100 K, and for  $x = 0.13$  the transition is almost synonymous with the Néel temperature. The  $x = 0.20$  sample has a single magnetic structure (type IA) present at all temperatures below the Néel temperature of  $115 \pm 2$  K. The ordered moments at 5 K in this region gradually decrease with an increase in sulfur content. For  $x = 0.20$ , the ordered moment at 5 K is  $(2.03 \pm 0.05) \mu_B$  per uranium atom.

The  $0 \leq x \leq 0.20$  regions may be summarized as follows (see Table I). The Néel temperatures and maximum ordered moments decrease by a small amount ( $\sim 10\%$ ) when diluted with 20% sulfur. The transition temperature from type I to type IA rises rapidly with increasing  $x$ , indicating the increasing stability of the type-IA magnetic structure. A similar situation exists in both the UP-US and UAs-Use system.<sup>11</sup>

#### B. Compositions $0.25 \leq x \leq 0.34$

In this region, samples with  $x = 0.25, 0.29, 0.30, 0.32,$  and  $0.34$  have been examined. Neutron-diffraction experiments<sup>4</sup> on  $UP_{0.75}S_{0.25}$  showed the presence of a long-range structure consisting of ferromagnetic layers of spins stacked in the sequence 5+, 4–, 5+, 4–, etc. This structure, and even more complex ones, may be viewed as a modulation of the magnetic moment along the  $c$  axis; the  $z$  component of the magnetic moment on the  $j$ th atom is described by

$$\mu_{jz} = \sum_{n=0}^{\infty} (A_n e^{i(\phi_n + \delta_n)} + A_n^* e^{-i(\phi_n + \delta_n)}), \quad (1)$$

where  $\phi_n = 2\pi n \vec{\tau} \cdot \vec{z}_j$ , and  $\delta_n$  is an arbitrary phase angle. The propagation direction is defined by  $\vec{\tau}$ , and the periodicity of the modulation is  $1/\tau$ . For every component of the modulation two satellites are present, situated at  $\pm n\tau$  and designated as  $hkl \pm n\tau$  from the nuclear reflections. The intensity of a particular satellite pair is proportional to the product of the coefficients  $A_n A_n^*$ . No information of the phase angles  $\delta_n$  can be obtained with diffraction techniques. The simplest structure of this type has a single component and is the ordering found in chromium metal. In Eq. (1), the  $z$  axis has been chosen as the propagation direction of the modulation for simplicity. The magnetic moments subtend an angle  $\beta$  with the propagation direction. In the special cases of  $\beta = 90$  or  $0^\circ$ , the wave structure is described as transverse or longitudinal, respectively. In chromium,<sup>17</sup> in which both types exist, the longitudinal wave (LW) is the stable



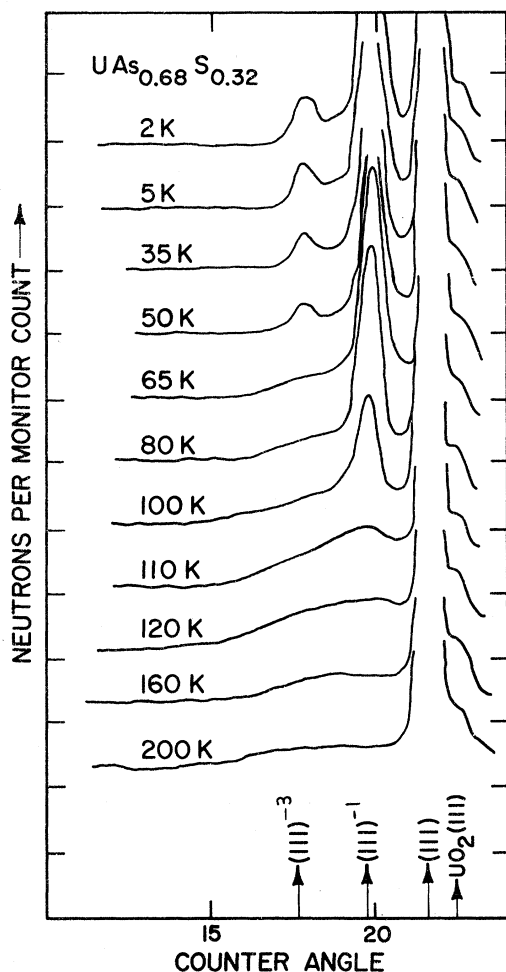


FIG. 3. Neutron-diffraction patterns of  $\text{UAs}_{0.68}\text{S}_{0.32}$  as a function of temperature. The intensity scale has been shifted vertically by one division for each step in temperature. The position of the first satellite for the LW phase ( $\tau = 0.285c^*$ ) is given by  $(111)^{-1}$ , and of the third satellite by  $(111)^{-3}$ .

tor of the LW decreases with an increase in sulfur concentration. For  $x = 0.32$ , the sample exhibits a single magnetic phase at all temperatures between  $T_N(108 \pm 2 \text{ K})$  and  $2.2 \text{ K}$ . For  $x = 0.34$ , a ferromagnetic contribution is observed below  $80 \text{ K}$ , and this LW magnetic structure has the smallest wave vector of  $(0.24 \pm 0.01)c^*$ . The diffraction patterns for all the LW phases are essentially the same, except for variations in the wave vector, and we shall describe the details only for the  $x = 0.32$  sample, which has the additional advantage of exhibiting a single magnetic phase. Figure 3 shows the experimental data for the angular region before the first nuclear reflection for a wide range of temperatures. As the sample is cooled, the critical scattering associated with the second-order transition at the Néel temperature increases. The Néel tempera-

ture is  $108 \pm 2 \text{ K}$ . At  $\sim 65 \text{ K}$ , an additional satellite is observed on the low-angle side of the  $(111)^{-1}$ , and may be indexed as  $(111)^{-3}$ .

An analysis of the linewidth of the  $(111)^{-1}$  satellite reflections indicates that the FWHM is  $0.72 \pm 0.03^\circ$ . This reflection occurs at  $2\theta = 19.77^\circ$ . The intrinsic peak shape, as determined from nuclear reflections, has a FWHM of  $0.62 \pm 0.02^\circ$  between  $2\theta$  values of  $17$  and  $23^\circ$ . The question then arises as to whether this 16% broadening can be due to sample inhomogeneity. Based on previous estimates,<sup>7</sup> we can expect that for  $\text{UAs}_{0.68}\text{S}_{0.32}$  the variation in sulfur concentration will be represented by  $x \pm 0.05x$ , i. e.,  $0.32 \pm 0.016$ . For  $x = 0.32$ ,  $\tau = (0.285 \pm 0.008)c^*$  and the variation of  $\tau$  over the LW phase is given approximately by  $d\tau/dx = -\frac{4}{3}$ . The wave vector should be represented by  $\tau = 0.285c^*$  with a spread  $\Delta\tau$  of  $\pm 0.021c^*$ . We have therefore convoluted such a Gaussian distribution describing the wave vector with the instrumental resolution function, which gives an FWHM of  $0.62^\circ$ , to determine the effect of sample inhomogeneity on the  $(111)^{-1}$  satellite reflection. For this value of  $\Delta\tau$ , however, the change in the peak shape is negligible. To obtain the observed FWHM by this method,  $\Delta\tau$  must be increased to  $0.15c^*$ , which implies a sulfur variation of  $0.12$ . Such a value is approximately eight times larger than the original estimate and is inconsistent with the sharpness of the high-angle x-ray lines. An alternative explanation of the difference between the magnetic and nuclear linewidths is to suppose that the degree of long-range order in the magnetic system is not as good as in the atomic lattice, which gives rise to the nuclear reflections. The LW modulation is therefore only coherent over relatively short lengths in the material.

The wave vector of the LW phase in  $\text{UAs}_{0.68}\text{S}_{0.32}$  is  $(0.285 \pm 0.008)c^*$ , and is independent of temperature (Fig. 3). At  $5 \text{ K}$  the amplitudes of the first and third harmonics are  $2.20$  and  $0.77\mu_B$  per uranium atom, respectively. The observed and calculated intensities are given in Table II. For this sample, the wave vector is indistinguishable from a commensurate structure with a wave vector of  $\frac{2}{7} = 0.2857c^*$ . Of course the wave vector is best determined if we can measure reflections such as  $(111)^{-3}$  that are well separated from their fundamental peak. Unfortunately, as Table II shows, the loss of sensitivity, primarily due to geometric factors in the powder technique, results in intensities too small to be observed. Whether the structure really becomes commensurate is of some importance and worth further consideration. First, we note that if  $\tau = \frac{2}{7}$  the second and fifth harmonics coincide in the diffraction pattern. [For example, the  $(111)^{-2}$  and  $(11\bar{1})^{+5}$  correspond

TABLE II. Observed and calculated intensities for  $\text{UAs}_{0.68}\text{S}_{0.32}$  at 5 K. Scattering lengths are  $b_U = 0.85$ ,  $b_{As} = 0.658$ , and  $b_S = 0.285$  (in units of  $10^{-12}$  cm); magnetic moments are  $2.20 \mu_B/\text{U}$  atom for the first harmonic and  $0.77 \mu_B/\text{U}$  atom for the third harmonic;  $q^2$  is the square of the magnetic interaction vector,  $f$  the magnetic form factor, and  $j$  the multiplicity.

$hkl$	$2\theta^\circ$	$(\sin\theta)/\lambda$	$j$	$q^2$	$f$	Calculated intensity	
						Nuclear	Magnetic
$(111)^{-3}$	17.75	0.125	8	0.990	0.92	$1.8 \pm 0.2$	1.8
$(111)^{-1}$	19.77	0.140	8	0.796	0.905	$9.5 \pm 0.3$	9.4
(111)	21.62	0.152	8			$13.2 \pm 0.3$	13.2
$(111)^{+1}$	23.85	0.168	8	0.548	0.87	$3.4 \pm 0.3$	4.1
(200)	24.98	0.178	6			$148 \pm 1$	148.5
$(200)^{+1}$	25.22	0.178	8	0.980	0.855	$8 \pm 2$	6.3
$(200)^{+3}$	27.18	0.191	8	0.845	0.835	$\sim 0.6$	0.5
$(202)^{-3}$	28.81	0.203	8	0.753	0.81	$< 0.5$	0.4
$(111)^{+3}$	29.17	0.205	8	0.368	0.81	$< 0.5$	0.2
$(113)^{-3}$	32.16	0.226	8	0.303	0.78	$< 0.5$	0.13
$(202)^{-1}$	32.99	0.232	8	0.576	0.77	$1.2 \pm 0.3$	1.8
(202)	35.48	0.249	12			$150 \pm 2$	151.8

to the same positions in reciprocal space.] At this position in Fig. 3 ( $2\theta = 18.45^\circ$ ) an upper limit of 0.4 (arbitrary units, but the same as used in Table II) may be put on the intensity of the second and fifth satellites, i. e.,  $I(111^{-2}) \leq 0.4$ . The amplitudes of a square-wave modulation require that the ratio of the fifth to third harmonics be 0.69. Inasmuch as  $I(111^{-3}) = 1.8 \pm 2$ , the implication is that  $I(111^{-2}) \approx 0.75$ . On the other hand, the ratio of the third to first harmonic amplitudes for a square wave is 0.357. The observed ratio is  $0.77/2.20 \approx 0.35$ , so that the first two harmonics are present in the correct proportions for a square-wave modulation. Second, we may consider that the magnitude of the magnetic moment, which is a well-defined quantity, is the same for all atoms in a commensurate structure. The value of  $I(111^{-1}) = 9.5$  corresponds to an ordered moment of  $1.74 \mu_B/\text{U}$  atom in a 4+, 3- configuration. This value is considerably lower than the trend in Table II would indicate and is even lower than found in US. By assuming a commensurate structure with a wave vector of  $\frac{2}{7}$ , we find, therefore, that the value of the localized moment is smaller than expected, and the predicted fifth-order satellite is not observed. A further point is that any commensurate structure that involves seven layers must have a small ferromagnetic component,<sup>18,19</sup> but with powder samples this would only contribute an additional 0.3 to the (111) nuclear reflection, and such a small amount cannot be detected reliably in addition to the (111) nuclear intensity of  $13.2 \pm 0.3$ . The rejection of the commensurate structure leaves a longitudinal modulation with a repeat of almost exactly  $3\frac{1}{2}$  unit cells. Although the amplitudes of the first and third harmonics are known, this does not specify the localized moments without a knowledge of the phase angles  $\delta$  in Eq. (1). However, we do not expect

the maximum amplitude to exceed  $\sim 2\mu_B$ , and, with harmonic amplitudes of 2.2 and  $0.77\mu_B$ , this is best achieved by arranging the amplitudes exactly out of phase, i. e.,  $|\delta_1 - \delta_2| = \pi$ . Under these conditions  $\mu_{\max} = 2.05\mu_B/\text{U}$  atom. A schematic picture of the LW is given in Fig. 4. At high

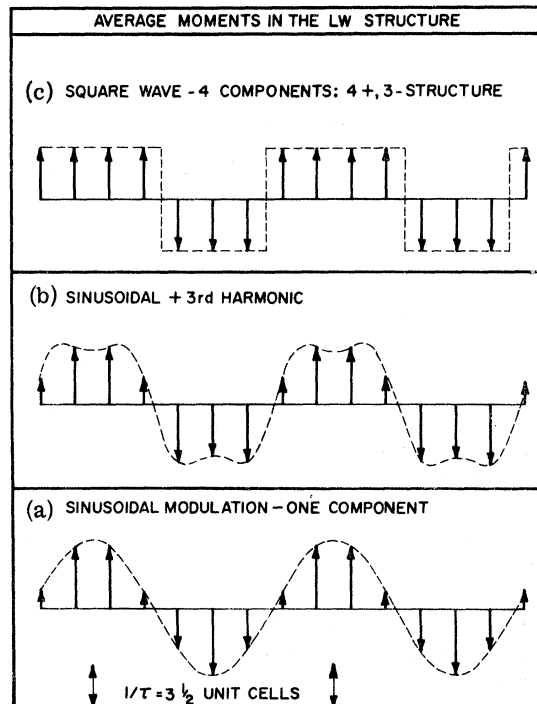


FIG. 4. Models for localized moments on uranium atoms. The structure is a longitudinal-wave arrangement rather than the transverse model drawn for convenience. (a) Simple sinusoidal arrangement, (b) sinusoidal plus third harmonic (as found in the UAs-US system), and (c) square-wave modulation 4+, 3-, etc., that requires an additional two components.

temperatures only a single component is present, as in Fig. 4(a). As the temperature is lowered the third harmonic develops and, if we assume the wave vector is exactly  $\frac{2}{7}$  and the phase difference is  $\pi$ , we get the picture of the localized moments as shown in Fig. 4(b). Such a modulation readily develops into the 4+, 3- arrangement if two more components, with the correct phase angles, are switched on. This is illustrated in Fig. 4(c).

The temperature dependence of the first and third harmonics is given in Fig. 5. The increase in amplitude on cooling below  $T_N$  is very rapid and does not fit any Brillouin function. For example, the first harmonic reaches  $\mu/\mu_{\max} = 0.9$  at  $T/T_c = 0.75$ , whereas the Brillouin function for  $S = \frac{1}{2}$ , which exhibits the fastest rise in  $\mu/\mu_{\max}$  with a decrease in temperature, reaches the same value of  $\mu/\mu_{\max}$  only at  $T/T_c = 0.60$ .

### C. Compositions $0.34 < x \leq 1.00$

As mentioned in Sec. II B for  $x = 0.34$  a ferromagnetic contribution is observed below 80 K. Following the magnetization<sup>21</sup> and neutron work<sup>3</sup> on the UP-US solid solutions, and the magnetization measurements on the UAs-USe solid solutions,<sup>22</sup> we can expect that over most of the phase diagram the ferromagnetic interaction dominates. The  $x = 0.34$  sample marks the beginning of this region in the UAs-US system, and the only other sample examined in this region (with  $x = 0.40$ ) is ferromagnetic throughout the ordered region. X-ray experiments<sup>21</sup> on the UP-US solid solutions indicate that, in samples with  $x \geq 0.75$ , the unit cell becomes rhombohedral at the Curie temperature.

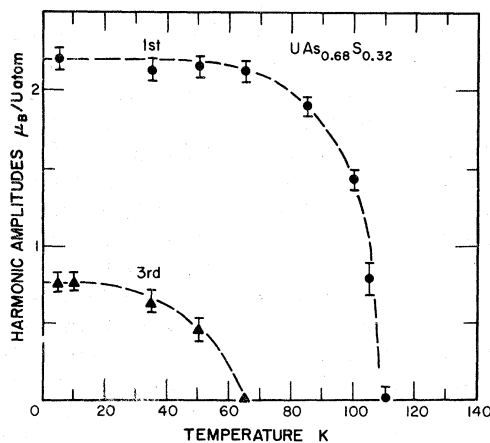


FIG. 5. Temperature dependence of the first and third harmonics for  $UAs_{0.68}S_{0.32}$ . These points are taken from the intensities of the  $(111)^{-1}$  and  $(111)^{-3}$  satellites, respectively.

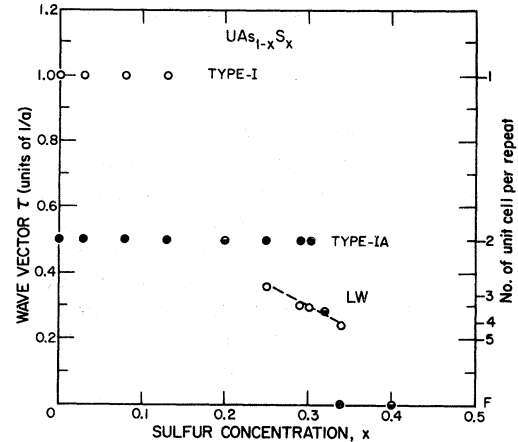


FIG. 6. Periodicities of the magnetic structure in the  $UAs_{1-x}S_x$  system as a function of sulfur concentration  $x$ . Open circles indicate the initial periodicity at  $T_N$ , closed circles the periodicity at 4.2 K, and half-filled circles a single value that applies to the material at all temperatures.

Similar experiments are planned on all the present samples.

The wave vectors observed in the UAs-US system are plotted in Fig. 6 as a function of sulfur concentration  $x$ . As noted earlier, the variation of  $\tau$  in the LW phase is almost linear with  $x$  and is given approximately by  $d\tau/dx = -\frac{4}{3}$ . The stability of the LW phase is limited to repeat distances between 2.8 and 4.2 unit cells. A tentative phase diagram of the UAs-US system is given in Fig. 7. The precise range of the LW is somewhat uncer-

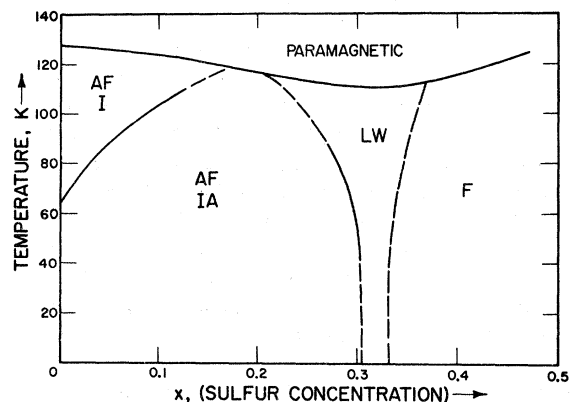


FIG. 7. Schematic magnetic phase diagram of the  $UAs_{1-x}S_x$  system as a function of sulfur concentration. Broken lines indicate that these phase boundaries are uncertain. The type-I structure is represented by AF I, the type IA by AF IA, the longitudinal-wave by LW, and ferromagnetism by F, which continues for  $x$  greater than 0.5.

tain and therefore marked with broken lines.

### III. DISCUSSION

During the preparation of this work for publication, accounts of magnetization<sup>23</sup> and neutron<sup>24</sup> experiments on the UAs-US system have been published. The magnetization results are interpreted by the authors as indicating ferromagnetism for  $x > 0.20$ . This is incorrect as indicated by both the authors' later neutron work<sup>24</sup> and the present study, and may be a result of not extending the magnetization measurements below 78 K. Another possibility, however, is that the LW phase is readily destroyed by the application of a magnetic field. Clearly, more detailed magnetization measurements extended to helium temperatures are required. The smooth variation of the effective moment and the Weiss constant ( $\theta_p$ ) are very similar to those reported for the UP-US system.<sup>21</sup> With respect to the neutron paper on the present system our results are in agreement with Ref. 24 for  $x \leq 0.20$ , the main conclusion being the rapid increase in stability of the type-IA structure as the sulfur concentration increases. For the interesting region  $0.25 \leq x \leq 0.35$ , one major and two minor discrepancies exist. Variations in composition probably explain the different wave vectors (0.36 and 0.40 $c^*$ ) reported for  $x = 0.25$ , and small differences over the position of the ferromagnetic boundary. Ferromagnetism is generally more reliably detected by magnetization measurements, although the response of the LW phase to an applied field should be determined before precise agreement between the two techniques can be expected. The most serious disagreement between the present work and Ref. 24, however, lies in their assignment of a commensurate 3+, 2- structure to compositions in the range  $0.25 \leq x \leq 0.35$ . Such an assignment is incompatible with our observation of a varying periodicity as a function of  $x$ . For example, in Fig. 3 the 3+, 2- configuration would result in a peak at  $2\theta = 18.92^\circ$ , which is midway between the positions marked  $(111)^{-3}$  and  $(111)^{-1}$ , and another peak  $\frac{1}{5}$  the size situated at the  $(111)^{-3}$  position. Our Fig. 3 shows that the third harmonic appears only at  $\sim 65$  K, whereas for the 3+, 2- configuration the ratio of the intensities of the first two satellites must be 5:1.

The transition in UP at 22 K that involves a sudden change in the ordered moment<sup>14</sup> has been discussed recently by Long and Wang<sup>16</sup> in terms of an electric-quadrupole interaction. The magnetic phase diagram of the UP-US system<sup>3</sup> shows that the transition in UP at 22 K persists in the phase diagram to about 10% sulfur concentration, but that its nature changes. Instead of a change

in the ordered moment only, the transition involves a change in the type of magnetic ordering, from type I to type IA. If two magnetic phases are present in unknown quantities, the neutron experiments cannot assign a unique value of the moment in a given structure. However, evidence from  $UP_{0.75}S_{0.25}$ ,<sup>4</sup> and our recent reexamination of  $UP_{0.90}S_{0.10}$ , UAs, and  $UAs_{1-x}S_x$  with  $x$  less than 0.10, suggest that the transformation to the type-IA structure is accompanied by a sharp increase in the magnitude of the magnetic moment. The mechanism proposed by Long and Wang essentially involves a transition between two discrete crystal-field energy levels. In UP the transition occurs at  $T/T_N = 0.17$ , whereas in UAs it occurs at  $T/T_N = 0.50$ , so that to extend the Long-Wang formalism to UAs, the magnitude of the electric-quadrupole interaction must be appreciably increased. A more serious objection is that by  $T/T_N \sim 0.5$ , the thermal population factors of the two closely separated crystal-field levels will effectively smear out any abrupt transition.

The influence of the crystal field in rare-earth pnictides and chalcogenides has received much attention recently.<sup>25,26</sup> The greater extent of the  $5f$  atomic wave functions implies that the crystal-field interactions in the actinide series are greater than those in the lanthanide series. For example, the parameter  $A_4 \langle r^4 \rangle$ , which is the dominating term in cubic materials, is estimated to vary between 10 and 100  $\text{cm}^{-1}$  in light rare-earth compounds<sup>26,27</sup> but is in the order of 2000  $\text{cm}^{-1}$  for the analogous actinide compounds.<sup>16,28</sup> Considerations of this large crystal-field potential lead to a breakdown of Russell-Saunders coupling, and calculations with intermediate coupling schemes should be attempted if the quantitative effects in these compounds are to be described. The simplest model for describing these actinide NaCl-structure compounds is one that assumes an integer number of  $f$  electrons on the actinide ion, and then proceeds with conventional crystal-field theory. Certainly the success of this model with the lanthanide chalcogenides and pnictides,<sup>25-27</sup> even for the light rare-earth elements, encourages this approach. The first such model, proposed by Grunzweig-Genossar *et al.*,<sup>1</sup> suggested a  $5f^2$  configuration. This has the disadvantage that the ground state is probably a singlet and the ordering must occur by exchange mixing with higher levels. The  $5f^2$  configuration does appear applicable in the case of UC, in which the susceptibility is temperature independent.<sup>29</sup> Chan and Lam<sup>28</sup> have proposed a  $5f^3$  configuration for the pnictides and  $5f^4$  for the chalcogenides. They have taken account of the large crystal fields and used intermediate coupling, but, rather surprisingly, the effective moment values are almost identical to

those derived using Russell-Saunders coupling. Neutron-diffraction experiments on single crystals of CeBi<sup>30</sup> and CeSb<sup>31</sup> have recently been reported, and similarities between the lanthanide compounds, especially those with cerium and neodymium, and the uranium compounds are becoming evident.

An alternative approach to the understanding of the electronic properties of these compounds is to assume that the 5*f* band intersects the Fermi surface, and that extensive band calculations are required to explain the magnetic behavior. Davis<sup>32</sup> has done some exploratory calculations along these lines, but more quantitative results are needed.

An important experiment that further emphasizes the need for the band approach is the photoemission work on US reported by Eastman and Kuznietz.<sup>33</sup> Although the spectra are rather complex, these workers conclude that the Fermi surface is located in a broad *f-d* band that is almost indistinguishable from the conduction band. The present neutron experiments suggest that a band approach is required for these compounds, but the unusual magnetic transitions and the fact that the spins are always parallel to the [100] direction in the antiferromagnetic compositions illustrate the importance of the crystal-field interactions.

\*Work performed under the auspices of the U. S. Atomic Energy Commission.

<sup>1</sup>J. Grunzweig-Genossar, M. Kuznietz, and F. Friedman, *Phys. Rev.* **173**, 562 (1968).

<sup>2</sup>G. T. Trammell, *Phys. Rev.* **131**, 932 (1963).

<sup>3</sup>M. Kuznietz, G. H. Lander, and Y. Baskin, *J. Appl. Phys.* **40**, 1130 (1969).

<sup>4</sup>G. H. Lander, M. Kuznietz, and D. E. Cox, *Phys. Rev.* **188**, 963 (1969).

<sup>5</sup>M. Kuznietz, Y. Baskin, and G. A. Matzkanin, *Phys. Rev.* **187**, 737 (1969).

<sup>6</sup>F. Friedman and J. Grunzweig-Genossar, *Phys. Rev. B* **4**, 180 (1971).

<sup>7</sup>M. Kuznietz, F. P. Campos, and Y. Baskin, *J. Appl. Phys.* **40**, 3621 (1969).

<sup>8</sup>R. Troc, A. Murasik, A. Zygmunt, and J. Leciejewicz, *Phys. Status Solidi* **23**, K123 (1967).

<sup>9</sup>J. Leciejewicz, A. Murasik, and R. Troc, *Phys. Status Solidi* **30**, 157 (1968).

<sup>10</sup>J. M. Williams, L. Heaton, and F. Campos, *J. Phys. Chem. Solids* **29**, 1702 (1968).

<sup>11</sup>J. Leciejewicz, A. Murasik, T. Palewski, and R. Troc, *Phys. Status Solidi* **38**, K89 (1970).

<sup>12</sup>Y. Baskin, *Trans. Met. Soc. AIME* **239**, 1708 (1967).

<sup>13</sup>Neutron Diffraction Commission, *Acta Cryst. A* **25**, 391 (1969); C. G. Shull (private communication).

<sup>14</sup>L. Heaton, M. H. Mueller, M. F. Adam, and R. L. Hitterman, *J. Appl. Cryst.* **3**, 289 (1970).

<sup>15</sup>S. L. Carr, C. Long, W. G. Moulton, and M. Kuznietz, *Phys. Rev. Letters* **23**, 786 (1969).

<sup>16</sup>C. Long and Y. L. Wang, *Phys. Rev. B* **3**, 1656 (1971).

<sup>17</sup>S. A. Werner, A. Arrott, and H. Kendrick, *Phys. Rev.* **155**, 528 (1967), and references therein.

<sup>18</sup>W. C. Koehler, J. W. Cable, E. O. Wollan, and

M. K. Wilkinson, *Phys. Rev.* **126**, 1672 (1962).

<sup>19</sup>T. O. Brun, S. K. Sinha, N. Wakabayashi, G. H. Lander, L. R. Edwards, and F. H. Spedding, *Phys. Rev. B* **1**, 1251 (1970).

<sup>20</sup>J. W. Cable, E. O. Wollan, W. C. Koehler, and M. K. Wilkinson, *Phys. Rev.* **140**, A1896 (1965).

<sup>21</sup>M. Allbutt, R. M. Dell, A. R. Junkison, and J. A. Marples, *J. Inorg. Nucl. Chem.* **32**, 2159 (1970).

<sup>22</sup>W. Trzebiatowski, A. Misiuk, and T. Palewski, *Bull. Acad. Polon. Sci. Ser. Sci. Chim.* **15**, 543 (1967).

<sup>23</sup>W. Trzebiatowski and T. Palewski, *Bull. Acad. Polon. Sci. Ser. Sci. Chim.* **19**, 83 (1971).

<sup>24</sup>J. Leciejewicz, A. Murasik, R. Troc, and T. Palewski, *Phys. Status Solidi* **46**, 391 (1971).

<sup>25</sup>P. Junod, A. Menth, and O. Vogt, *Physik Kondensierten Materie* **8**, 323 (1969).

<sup>26</sup>Y. L. Wang and B. R. Cooper, *Phys. Rev. B* **2**, 2607 (1970).

<sup>27</sup>K. C. Turberfield, L. Passell, R. J. Birgeneau, and E. Bucher, *Phys. Rev. Letters* **25**, 752 (1970).

<sup>28</sup>S. K. Chan and D. J. Lam, in *Plutonium 1970 and Other Actinides*, edited by W. N. Miner (American Institute of Mining, Metallurgical, and Petroleum Engineers, New York, 1970), Vol. 1, p. 219.

<sup>29</sup>C. H. de Novion and P. Costa, *Compt. Rend.* **B270**, 1415 (1970).

<sup>30</sup>J. W. Cable and W. C. Koehler, in *Magnetism and Magnetic Materials*, No. 5, edited by C. D. Graham and J. J. Rhyne (AIP, New York, 1972), p. 1381.

<sup>31</sup>B. Lebech, P. Fischer, and B. D. Rainford, in *Rare Earths and Actinides* (The Institute of Physics, London, 1971), p. 204.

<sup>32</sup>H. L. Davis, in Ref. 31, p. 126.

<sup>33</sup>D. E. Eastman and M. Kuznietz, *Phys. Rev. Letters* **26**, 846 (1971).